



Nonlinear Optical Properties of Materials

Howard R. Schlossberg
Raymond V. Wick
Chairs/Editors

10-11 August 1989
San Diego, California



Volume 1148

Nonlinear Optical Properties of Materials

Howard R. Schlossberg
Raymond V. Wick
Chairs/Editors

10–11 August 1989
San Diego, California

Sponsored by
SPE—The International Society for Optical Engineering

Cooperating Organizations
Applied Optics Laboratory/New Mexico State University
Center for Applied Optics/University of Alabama in Huntsville
Center for Applied Optics Studies/Rose-Hulman Institute of Technology
Center for Electro-Optics/University of Dayton
Center for Excellence in Optical Data Processing/Carnegie Mellon University
Jet Propulsion Laboratory/California Institute of Technology
Optical Sciences Center/University of Arizona
Optoelectronic Computing Systems Center/University of Colorado,
Colorado State University

Published by
SPE—The International Society for Optical Engineering
P.O. Box 10, Bellingham, Washington 98227-0010 USA
Telephone 206/676-3290 (Pacific Time) • Telex 46-7053



Volume 1148



The papers appearing in this book comprise the proceedings of the meeting mentioned on the cover and title page. They reflect the authors' opinions and are published as presented and without change, in the interests of timely dissemination. Their inclusion in this publication does not necessarily constitute endorsement by the editors or by SPIE.

Please use the following format to cite material from this book:

Author(s), "Title of Paper," *Nonlinear Optical Properties of Materials*, Howard R. Schlossberg, Raymond V. Wick, Editors, Proc. SPIE 1148, page numbers (1990).

Library of Congress Catalog Card No. 89-43261
ISBN 0-8194-0184-6

Copyright © 1990, The Society of Photo-Optical Instrumentation Engineers.

Copying of material in this book for sale or for internal or personal use beyond the fair use provisions granted by the U.S. Copyright Law is subject to payment of copying fees. The Transactional Reporting Service base fee for this volume is \$2.00 per article and should be paid directly to Copyright Clearance Center, 27 Congress Street, Salem, MA 01970. For those organizations that have been granted a photocopy license by CCC, a separate system of payment has been arranged. The fee code for users of the Transactional Reporting Service is 0-8194-0184-6/90/\$2.00.

Individual readers of this book and nonprofit libraries acting for them are permitted to make fair use of the material in it, such as to copy an article for teaching or research, without payment of a fee. Republication or systematic or multiple reproduction of any material in this book (including abstracts) is prohibited except with the permission of SPIE and one of the authors.

Permission is granted to quote excerpts from articles in this book in other scientific or technical works with acknowledgment of the source, including the author's name, the title of the book, SPIE volume number, page number(s), and year. Reproduction of figures and tables is likewise permitted in other articles and books provided that the same acknowledgment of the source is printed with them, permission of one of the original authors is obtained, and notification is given to SPIE.

In the case of authors who are employees of the United States government, its contractors or grantees, SPIE recognizes the right of the United States government to retain a nonexclusive, royalty-free license to use the author's copyrighted article for United States government purposes.

Address inquiries and notices to Director of Publications, SPIE, P.O. Box 10, Bellingham, WA 98227-0010 USA.

NONLINEAR OPTICAL PROPERTIES OF MATERIALS

Volume 1148

CONFERENCE COMMITTEE

Chairs

Howard R. Schlossberg, Air Force Office of Scientific Research
Raymond V. Wick, Air Force Weapons Laboratory

Cochairs

Ian C. McMichael, Rockwell International Science Center
James R. Rotgé, Frank J. Seiler Research Laboratory
Duncan G. Steel, University of Michigan

Session Chairs

Session 1—Photorefractive Materials and Characterization
Ian C. McMichael, Rockwell International Science Center

Session 2—Nonlinear Optical Semiconductor Materials
Duncan G. Steel, University of Michigan

Session 3—Nonlinear Optical Fibers and Waveguides
James R. Rotgé, Frank J. Seiler Research Laboratory

Conference 1148, *Nonlinear Optical Properties of Materials*, was part of a four-conference program on materials held at SPIE's 33rd Annual International Symposium on Optical & Optoelectronic Applied Science & Engineering, 6–11 August 1989, San Diego, California. The other conferences were

Conference 1146, *Diamond Optics II*

Conference 1147, *Nonlinear Optical Properties of Organic Materials II*

Conference 1149, *Optical Materials Technology for Energy Efficiency and Solar Energy Conversion VIII*

Program Chair: **Robert Schwartz**, Naval Weapons Center

INTRODUCTION

Nonlinear optics has been an active research field since the classic work of Peter Franken soon after the first demonstrations of the laser. Recently, however, the field has become much more active, and the breadth of both research and applications has greatly enlarged. Important functions under investigation include switching, frequency conversion, and phase conjugation, for applications including communications, computing, image amplification and processing, and laser beam phase correction and control.

Fundamental to research in and applications of nonlinear optics are nonlinear optical materials. The availability of suitable materials will often determine whether an application is a pipe dream, a laboratory trick, or something practical and useful. The demands placed on a nonlinear optical material depend on the particular application, but, in general, they are very stringent. Requirements include large nonlinearity, often with low absorption and high speed (usually a contradictory set), good optical and mechanical properties, and no unwanted changes (damage) in response to the optical radiation to which the material is subject.

The purpose of this conference was to review the status of research on several of the most promising classes of nonlinear optical materials: photorefractives, semiconductors, and fibers, both crystalline and glass. Another major class of nonlinear optical materials—the organics—was the subject of another conference (Conference 1147) at this SPIE symposium.

The session on photorefractive materials featured a presentation on progress in growth and applications of new tungsten bronze materials, and included presentations on aspects of hologram storage and nonlinear phase conjugation.

The semiconductor session included presentations on large nonlinearities by resonant and by charge-transport enhancement, several presentations on photorefractive effects in semiconductors, and several presentations on the study and use of exciton nonlinearities in quantum-well structures.

The nonlinear optical fibers session featured presentations on second-harmonic generation in glass fibers—a poorly understood but potentially very important process. There were several theories to explain the overall phenomenon, as well as a theory to show how the process begins. The session also featured a presentation on nonlinear frequency conversion in lithium niobate fibers and films, whose ferroelectric domains have been periodically poled in order to provide quasi-phases matching.

We particularly wish to thank the cochairs who actually organized the sessions, Ian McMichael, Duncan Steel, and Jim Rotgé. The success of the conference is their doing.

Howard R. Schlossberg

Air Force Office of Scientific Research

Raymond V. Wick

Air Force Weapons Laboratory

NONLINEAR OPTICAL PROPERTIES OF MATERIALS

Volume 1148

CONTENTS

	Conference Committee	v
	Introduction	vi
SESSION 1	PHOTOREFRACTIVE MATERIALS AND CHARACTERIZATION	
1148-01	Photorefractive tungsten bronze materials and applications (Invited Paper) R. R. Neurgaonkar, W. K. Cory, J. R. Oliver, Rockwell International Science Ctr.; E. J. Sharp, M. J. Miller, G. L. Wood, W. W. Clark, III, A. G. Mott, G. J. Salamo, B. D. Monson, Army Ctr. for Night Vision and Electro-Optics.	2
1148-02	Photorefractive properties of Cr-doped single-crystal strontium barium niobate K. Sayano, A. Yariv, California Institute of Technology; R. R. Neurgaonkar, Rockwell International Science Ctr.	7
1148-03	Effects of applied voltage on holographic storage in SBN:60 J. E. Ford, Y. Taketomi, S. H. Lee, Univ. of California/San Diego; D. Bize, Centre d'Etudes et de Recherches de Toulouse (France); R. R. Neurgaonkar, Rockwell International Science Ctr.; S. Y. Fainman, Univ. of Michigan.	12
1148-04	Phase conjugation in BaTiO₃ at 830 nm I. Bendall, D. M. Gookin, Naval Ocean Systems Ctr.	25
1148-05	Recording of frequency-difference holograms in lithium niobate S. Fries, J. Otten, K. H. Ringhofer, R. A. Rupp, Univ. Osnabrück (FRG).	30
1148-06	Z-scan: a simple and sensitive technique for nonlinear-refraction measurements M. Sheik-bahae, A. A. Said, T. Wei, Y. Wu, D. J. Hagan, M. J. Soileau, E. W. Van Stryland, CREOL/Univ. of Central Florida.	41
1148-07	Photorefractive properties of KTa_{1-x}Nb_xO₃ in the paraelectric phase A. J. Agranat, V. Leyva, K. Sayano, A. Yariv, California Institute of Technology.	52
1148-08	Persistent internal-polarization characteristics of photorefractive barium titanate monocrystal P. K. Pillai, J. J. Lew, A. Gavrielides, C. M. Clayton, A. Corvo, Air Force Weapons Lab.	67
1148-09	Theory of photorefractive nonlinear effects in a self-pumped phase conjugator P. M. Petersen, Technical Univ. of Denmark (Denmark).	79
1148-25	Low-temperature pulsed plasma deposition: Part 4: preparation of layered structures of amorphous chalcogenide glasses with nonlinear optical properties I. P. Llewellyn, G. Scarsbrook, R. A. Heinecke, STC Technology Ltd. (UK).	84
SESSION 2	NONLINEAR OPTICAL SEMICONDUCTOR MATERIALS	
1148-10	Large, fast, free-electron-induced optical nonlinearities (Invited Paper) P. A. Wolff, NEC Research Institute; S. Y. Auyang, Massachusetts Institute of Technology.	98
1148-11	Magnetic susceptibility of the 2-D electrons of small-gap semiconductors having nonlinear optical properties K. P. Ghatak, A. Ghoshal, Jadavpur Univ. (India); S. N. Biswas, Bengal Engineering College (India).	108

(continued)

NONLINEAR OPTICAL PROPERTIES OF MATERIALS

Volume 1148

1148-12	Quasi-resonant optical nonlinearities and exciton dephasing in CdS (Invited Paper) M. Dagenais, Univ. of Maryland.	120
1148-13	Subpicosecond all-optical modulation using the optical Stark effect in a nonlinear directional coupler (Invited Paper) J. P. Sokoloff, P. A. Harten, R. Jin, C. Chuang, M. E. Warren, H. M. Gibbs, S. G. Lee, N. Peyghambarian, Univ. of Arizona.	132
1148-14	Exciton ionization of InGaAs quantum wells (Invited Paper) I. Bar-Joseph, Weizmann Institute of Science (Israel); M. Wegener, T. Y. Chang, D. S. Chemla, AT&T Bell Labs.	136
1148-15	Photorefractive effects in semiconductors for deep-level spectroscopy (Invited Paper) G. C. Valley, Hughes Research Labs.	142
1148-16	Charge-transport-enhanced optical nonlinearities in semiconductors (Invited Paper) A. R. Kost, E. Garmire, Univ. of Southern California; T. Hasenberg, Hughes Research Labs.	144
1148-17	Excitonic effects in lattice-matched and strained quantum wells and their application to optical devices (Invited Paper) P. K. Bhattacharya, Univ. of Michigan.	152
SESSION 3	NONLINEAR OPTICAL FIBERS AND WAVEGUIDES	
1148-18	Saturation of nonlinearities and waveguide device implications (Invited Paper) G. Assanto, J. P. Sabini, N. Finlayson, G. I. Stegeman, Univ. of Arizona; S. Trillo, S. Wabnitz, Fondazione Ugo Bordoni (Italy).	162
1148-19	Theory for efficient second-harmonic generation and the formation of Hill gratings in germanosilicate fibers N. M. Lawandy, Brown Univ.	175
1148-20	Efficient second-harmonic generation in glass fibers: the possible role of photoinduced charge redistribution D. Z. Anderson, Univ. of Colorado and National Institute of Standards and Technology.	186
1148-21	Frequency-doubling via quadrupole and dipole-interface interactions in optical glass fibers W. M. Henry, Univ. of Arizona; U. Osterberg, U.S. Air Force Academy.	197
1148-23	Crystal-cored fiber using organic material and focusing properties of generated second-harmonic wave T. Uemiyu, N. Uenishi, Y. Shimizu, Sumitomo Electric Industries, Ltd. (Japan); S. Okamoto, K. Chikuma, T. Tohma, Pioneer Electronical Corp. (Japan); S. Umegaki, Tokyo Engineering Univ. (Japan).	207
1148-24	Quasi-phase-matched interactions in lithium niobate (Invited Paper) M. M. Fejer, G. A. Magel, E. J. Lim, Stanford Univ.	213
	Author Index	225

NONLINEAR OPTICAL PROPERTIES OF MATERIALS

Volume 1148

SESSION 1

Photorefractive Materials and Characterization

Chair

Ian C. McMichael

Rockwell International Science Center

Photorefractive tungsten bronze materials and applications

R.R. Neurgaonkar, W.K. Cory and J.R. Oliver

Rockwell International Science Center
Thousand Oaks, CA 91360

and

E.J. Sharp, M.J. Miller, G.L. Wood, W.W. Clark III, A.G. Mott, G.J. Salamo and B.D. Monson

Center for Night Vision and Electro-Optics
Fort Belvoir, VA 22060-5677

ABSTRACT

We review the current status of the photorefractive tungsten bronze ferroelectric crystals in terms of their electro-optic character and applications, with special emphasis on the current results for doped SBN:60 crystals. New results pertaining to phase conjugation and double phase conjugation (Bridge Conjugator) and the effects of internal fields on beam fanning are discussed.

1. INTRODUCTION

The need for optical materials with high coupling coefficients and fast response times for photorefractive applications such as phase conjugation, optical computing, image processing and laser hardening has stimulated work on doped tungsten bronze (T.B.) ferroelectric crystals. Several T.B. solid solutions such as $\text{Sr}_{1-x}\text{Ba}_x\text{Nb}_2\text{O}_6$ (SBN), $\text{Ba}_{2-x}\text{Sr}_x\text{K}_{1-y}\text{Na}_y\text{Nb}_5\text{O}_{15}$ (BSKNN) and $\text{Sr}_{2-x}\text{Ca}_x\text{NaNb}_5\text{O}_{15}$ (SCNN) have been found to be suitable for photorefractive applications because their optical figure-of-merit ($n^3 r_{ij}/\epsilon$) is comparable to, or better than, other leading material such as BaTiO_3 , KNbO_3 , LiNbO_3 , and BSO.¹⁻⁴ Since bronze crystals offer a wide range of electro-optic constants and the structural flexibility to accommodate dopants in more than one crystallographic site, these crystals are being actively investigated for photorefractive applications in our work. This paper reports the growth and classification of T.B. materials for these applications.

2. IMPORTANCE OF TUNGSTEN BRONZE CRYSTALS

Photorefractive effects have been observed in a variety of electro-optic materials such as BaTiO_3 , KTN, LiNbO_3 , LiTaO_3 , CdS, BSO, BGO, BTO, $\text{Ba}_2\text{NaNb}_5\text{O}_{15}$, BSKNN and SBN.¹⁻⁶ Depending on the band gap in a given material, refractive index changes may be induced not only by visible light, but also by ultraviolet and IR radiation. Among these key photorefractive materials, oxide ferroelectric crystals are being extensively studied because they exhibit large electro-optic coefficients and large photorefractive coupling. Currently, we are exploring various tungsten bronze host crystals for photorefractive applications because of the following important features:

1. Longitudinal (r_{51}) and transverse (r_{33}) electro-optic effects can be made large according to device requirements.
2. High coupling and fast response can be attained in the desired spectral range by the use of the 15-, 12-, 9- and 6-fold coordinated lattice sites for a given dopant.
3. On cooling, the longitudinal electro-optic response increases in BSKNN and SCNN, thereby enhancing the potential of these crystals for device applications.
4. Photorefractive speed can be dramatically increased by the application of an external field.
5. Gratings can be written in two different directions simultaneously using different r_{ij} in BSKNN and SCNN crystals.

3. CLASSIFICATION AND GROWTH OF BRONZE CRYSTALS

The tungsten bronze compositions can be represented by the general formulas $(\text{A}_1)_4(\text{A}_2)_2\text{C}_4\text{B}_{10}\text{O}_{30}$ and $(\text{A}_1)_4(\text{A}_2)_2\text{B}_{10}\text{O}_{30}$, in which A_1 , A_2 , C and B are 15-, 12-, 9- and two 6-fold coordinated sites in the crystal structure. The ferroelectric phases can be divided into two groups: those with tetragonal symmetry (4 mm), which are ferroelectric, and those with orthorhombic symmetry (mm2), which are both ferroelectric and ferroelastic. In the orthorhombic structure, the polar axis can be either along the c-axis, such as in $\text{Sr}_{2-x}\text{Ca}_x\text{NaNb}_5\text{O}_{15}$ (SCNN) or $\text{Ba}_2\text{NaNb}_5\text{O}_{15}$, or along the a- or b-axis, such as in PbNb_2O_6 , and $\text{Pb}_2\text{KNb}_5\text{O}_{15}$. These tetragonal and orthorhombic groups are further subgrouped according to crystal symmetry and the longitudinal and transverse ferroelectric and optical properties,

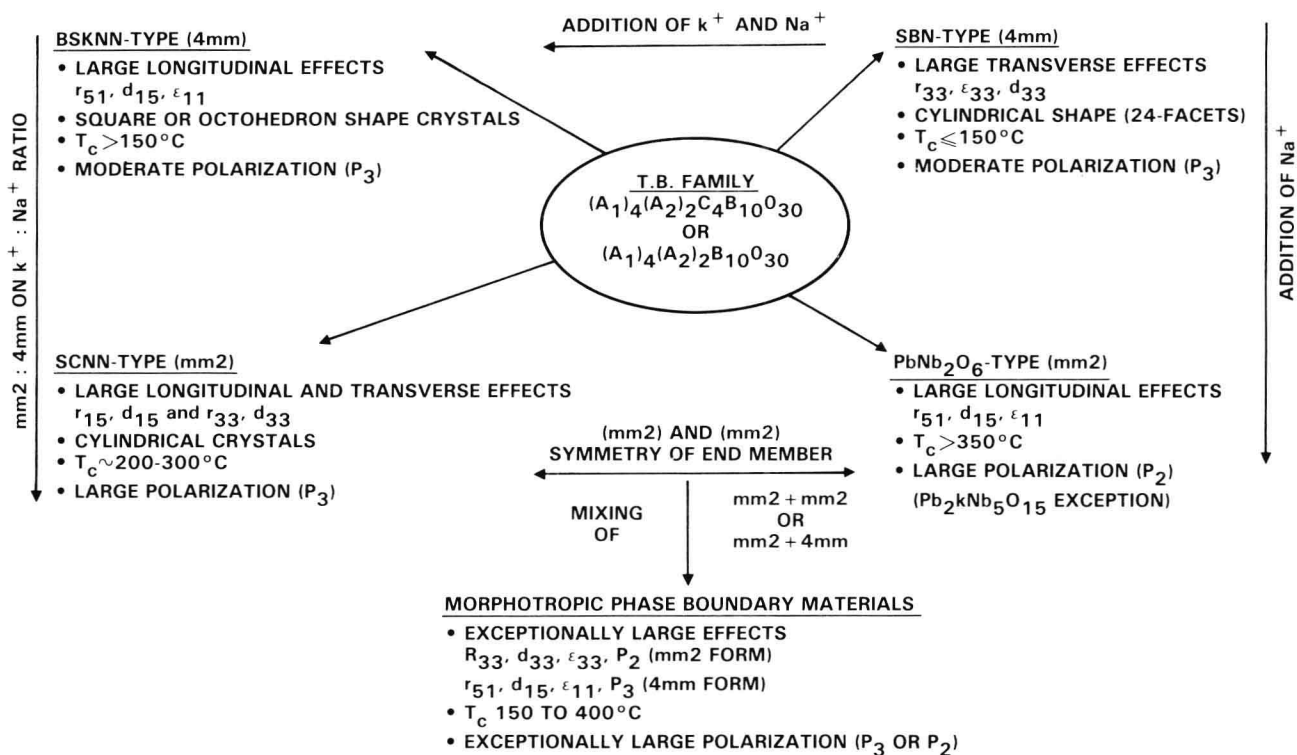


Figure 1. Classification of tungsten bronze crystals based on their ferroelectric and electro-optic character.

as summarized in Figure 1. These properties are distinguishable only in single crystals of each type,⁷ as it is very difficult to recognize these differences in polycrystalline ceramic materials.

The photorefractive studies described in this paper were carried out in three different tungsten bronze hosts, namely $\text{Sr}_{1-x}\text{Ba}_x\text{Nb}_2\text{O}_6$ (SBN), $\text{Ba}_{2-x}\text{Sr}_x\text{K}_{1-y}\text{Na}_y\text{Nb}_5\text{O}_{15}$ (BSKNN) and $\text{Sr}_{2-x}\text{Ca}_x\text{NaNb}_5\text{O}_{15}$ (SCNN), which exemplify the different types electro-optic response available in this crystal family (Figure 2). These crystals were grown by the Czochralski technique using an rf induction furnace and platinum crucibles.^{5,6} Among these crystals, $\text{Sr}_{0.6}\text{Ba}_{0.4}\text{Nb}_2\text{O}_6$ (SBN:60) was easier to grow since this composition is believed to exist near the congruent melting region.⁸ Currently, we have been able to grow SBN single crystals over 2.5 cm in diameter while other crystals based on BSKNN and SCNN are being grown over 1 cm diameter. The growth procedures are discussed in earlier papers.⁵⁻⁸

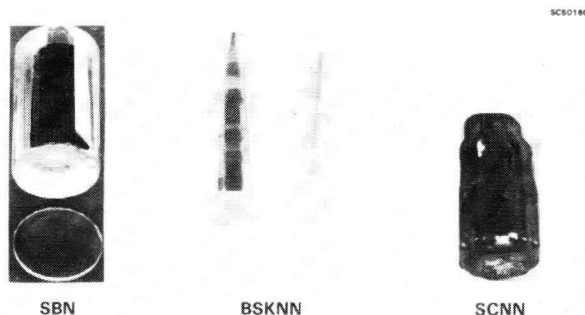


Figure 2. Photorefractive tungsten bronze single crystals.

SBN crystals are tetragonal at room temperature for all Ba:Sr ratios with the polar axis oriented along $\langle 001 \rangle$. SBN crystals exhibit strong transverse ferroelectric and optical effects such as the polar axis dielectric constant ϵ_{11} , the linear electro-optic coefficient r_{33} , the piezoelectric constant d_{33} , and electromechanical coupling K_{33} . BSKNN crystals show strong longitudinal effects such as ϵ_{11} , r_{51} , d_{15} , K_{15} , even though the polar axis remains along $\langle 001 \rangle$. The BSKNN-1 and BSKNN-2 compositions have ferroelectric, optical and

photorefractive characteristics similar to BaTiO₃. The smaller unit cell BSKNN-3 and BSKNN-5 compositions are pseudo-tetragonal at room temperature and they exhibit moderately large r_{51} and r_{33} . In orthorhombic SCNN crystals, both r_{51} and r_{33} are large and nearly equal. Furthermore, SCNN has a spontaneous polarization, P_3 , almost 25% higher than in SBN; hence, the optical figure-of-merit for SCNN, $n^3 r_{ij} / \epsilon$, for SCNN is significantly higher than that for SBN or BaTiO₃. Because of the availability of two large electro-optic coefficients, it may be possible to write gratings in two different directions simultaneously in BSKNN and SCNN crystals. This is a rare advantage which could be significant for optical computing and 3-D storage.

The photorefractive properties of doped SBN:60 are presented in Table 1. An important feature of SBN crystals is that the photorefractive properties, such as speed and coupling, depend on the type of dopant and its site preference in tungsten bronze crystal structure. For example, Ce³⁺ in the 12-fold coordinated site has response in visible with coupling as high as 45 cm⁻¹ (plate) and response times of 10 - 40 ms at 2 W/cm². On the other hand, Cr³⁺-doped SBN:60 crystals have a spectral response which extends out to 1.0 μ m and response times almost an order of magnitude faster than Ce³⁺-doped crystals. However, the coupling coefficient for Cr³⁺-doped crystals is considerably lower at 6 cm⁻¹. As shown in Figure 3, we have established the trends of dopants with respect to their site occupancies in the T.B. structure and using these criteria, it should be possible to further control the speed and coupling in the desired spectral range.

Table 1 Preliminary Photorefractive Results for Different Dopants

PROPERTY	Ce ³⁺ -DOPED SBN:60		Cr ³⁺ -DOPED SBN:60	Fe ³⁺ -DOPED SBN:60
	12-FOLD	9-FOLD	6-FOLD	6-FOLD
CRYSTAL COLOR	PINK	GREENISH-YELLOW	GREENISH-YELLOW	YELLOW
QUALITY	EXCELLENT	EXCELLENT	EXCELLENT	REASONABLE*
ELECTRO-OPTIC COEFFICIENT $\times 10^{-12}$ mV	460	460	550	480
BEAM FANNING RESPONSE				
AT 40 mW/cm ²	2.5s	3.0s	0.7s	2.8s
AT 0.2 W/cm ²	0.6s	1.2s	—	—
AT 2 W/cm ²	0.05s	0.09s	0.008s	0.07s
COUPLING COEFFICIENT	~ 19 cm ⁻¹ (CUBE) ~ 45 cm ⁻¹ (PLATE)	$\sim 5-6$ cm ⁻¹	$\sim 6-7$ cm ⁻¹	—
SPECTRAL RESPONSE	0.4-0.7 μ m	0.4-0.9 μ m	0.6-1.0 μ m	0.4-0.9 μ m
SPPCR	EXCELLENT	EXCELLENT	EXPECTED	EXPECTED

*STRIATED AT HIGHER DOPING LEVELS

Two new effects have been discovered using a Ce³⁺-doped SBN:60 crystal.⁹ First, high intensity multicolored isotropic conical diffraction rings are formed when the crystal is inserted into a multiline argon-ion laser beam. The origin of this effect is Bragg scattering from self-induced photorefractive gratings. When the multicolored rings were reflected into the crystal, phase conjugates of all eight laser lines were produced in a time very near to the beam fanning response time.¹⁰ Second, self-pumped phase conjugation via internal reflection¹¹ has been demonstrated at several different simultaneous wavelengths by spatially separating the argon-ion laser lines with dispersing elements. Figure 4 shows the experimental set-up used to observe multicolored self-pumped phase conjugation in SBN:60.⁹

A new method for double phase conjugation has been discovered which is particularly suited to tungsten bronze SBN.¹² The same method was also used to produce conjugate waves in BaTiO₃ and BSKNN crystals. This new arrangement is highly insensitive to the alignment of the two incident beams. This is due in part to the fact that in this geometry none of the beams are required to undergo reflections within the crystal. This new double-phase conjugate mirror quickly forms a conjugate image with high reflectivity and fidelity and is free from instabilities due to frequency shifts or competition from self-pumping. Figure 5 shows a sketch of this double phase conjugator which is called a "bridge conjugator" because the two input beams are observed to bridge together via beam fanning and overlap within the

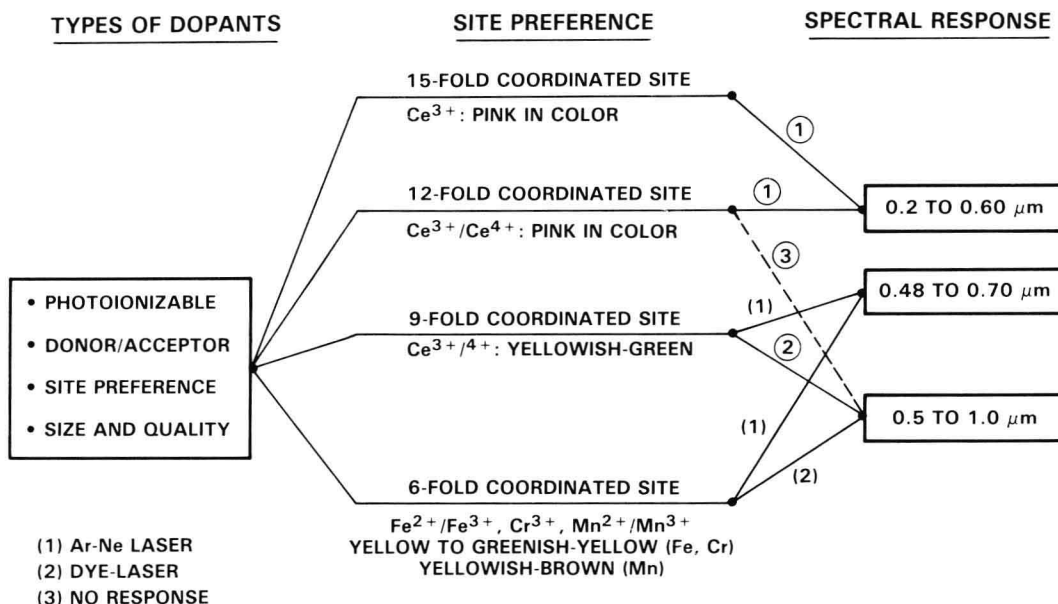


Figure 3. Role of dopants for photorefractive applications.

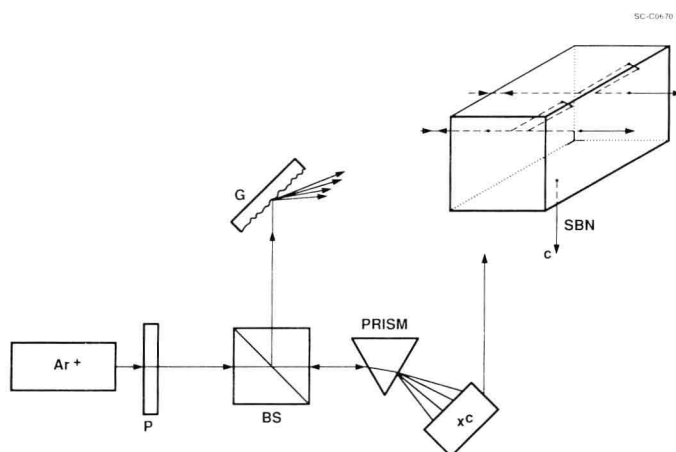


Figure 4. Diagram of the experimental apparatus for simultaneous self-pumping at several colors. The crystal c-axis points into the page so that light bends toward the top of the crystal with each color forming an independent loop at the upper right hand edge of the crystal (see insert of SBN crystal).

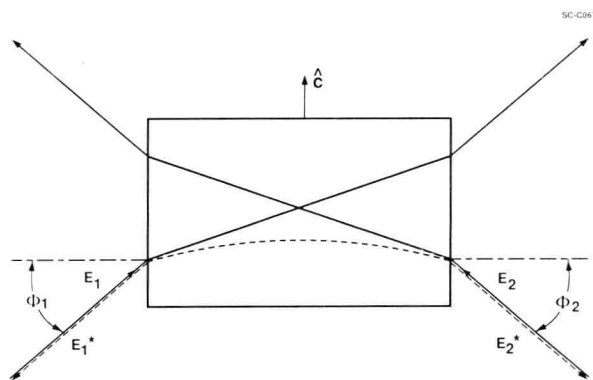


Figure 5. Sketch of a double phase conjugator in the "bridge conjugator" geometry. E_1 and E_2 are the incident optical electromagnetic fields, while E_1^* and E_2^* are the corresponding conjugate fields. Both beams are required for either conjugate to exist and the energy for the conjugate of one beam is supplied by the other beam.

crystal without reflecting off a crystal face. Applications for the bridge conjugator are image addition and subtraction, communications and reconfigurable interconnects.

Significant increases ($\times 10$) in both speed and gain of the photorefractive beam fanning process have been obtained via three different methods in SBN and BSKNN.¹³ These methods involve the creation of a DC electric field either (1) externally, (2) by the pyroelectric effect, or (3) by thermally cycling the crystals in the presence of laser radiation. Enhanced effects have been observed for both ordinary and extraordinary polarized light. Figure 6 provides a comparison of the on-axis beam depletion for normal beam fanning and the enhanced effects. All three methods gave similar results and are shown here for ordinary polarized light for an SBN crystal. Optical limiters, associative holographic memories, and the real-time image processing are obvious applications.

Self-pumped phase conjugation via internal reflection in a photorefractive medium produced by a series of intense nanosecond pulses was recently demonstrated.¹⁴ This is the first report of short-pulse induced self-pumped phase conjugation in a photorefractive

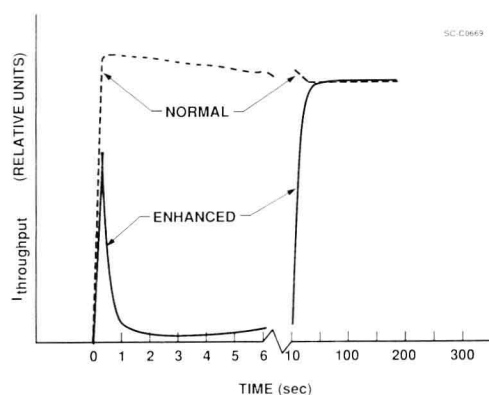


Figure 6. This figure shows the typical behavior of beam fanning which is enhanced by DC electric fields generated by any of the three methods. In this plot the intensity of light passing through the crystal is measured with an apertured detector (y-axis) as a function of elapsed time (x-axis).

medium, Fifteen picosecond pulses at 532 nm from a YAG laser ranging in intensity from 9×10^4 to 9×10^5 W/cm² have been used. Three experiments have been conducted using a crystal of Rh³⁺-doped SBN:60. The conjugate signal began with the first pulse and the time to reach 63% of its equilibrium value scaled as the inverse of the square of the intensity (I^{-2}). The measured equilibrium conjugate reflectivity was 29%.

In conclusion, tungsten bronze SBN and BSKNN crystals appear to be very promising for future photorefractive applications in phase conjugation, optical computing and image processing. Host crystal-dopant interactions will continue to be an important area of research in the bronze ferroelectrics in order to maximize the relevant photorefractive properties for these applications.

4. ACKNOWLEDGEMENT

This work was supported under DARPA Contract No. DAAB07-88-C-E243.

5. REFERENCES

1. P. Gunter, *Physics Reports*, **92**(4), 199 (1982).
2. M. Peltier and F. Micheron, *J. Appl. Phys.* **48**, 3683 (1977).
3. J.J. Amodei, D.L. Staebler and A.W. Stephens, *Appl. Phys. Lett.* **18**, 507 (1971).
4. J.B. Thaxter, *Appl. Phys. Lett.* **15**, 210 (1969).
5. R.R. Neurgaonkar and W.K. Cory, *J. Opt. Soc. Am. B* **3**(2), 274 (1986).
6. R.R. Neurgaonkar, W.K. Cory, J.R. Oliver, M.D. Ewbank and W.F. Hall, *J. Opt. Engineering*, **26**(5), 392 (1987).
7. R.R. Neurgaonkar, W.K. Cory, J.R. Oliver, M. Khoshnevisan and E.J. Sharp, to be published in *Ferroelectrics*.
8. R.R. Neurgaonkar, W.K. Cory, J.R. Oliver, E.J. Sharp, M.J. Miller, G.L. Wood and W.W. Clark III, *J. Cryst Growth*, **84**, 629 (1987).
9. G.J. Salamo, M.J. Miller, W.W. Clark III, G.L. Wood, E.J. Sharp and R.R. Neurgaonkar, *Opt. Soc. Am. Tech. Digest on Lasers and Electro-Optics*, **60** (1988).
10. G.J. Salamo, M.J. Miller, W.W. Clark III, G.L. Wood, E.J. Sharp and R.R. Neurgaonkar, *Appl. Opt.* **27**, 4356 (1988).
11. J. Feinberg, *Opt. Lett.* **7**, 486 (1982).
12. E.J. Sharp, W.W. Clark III, M.J. Miller, G.L. Wood, B.D. Monson, G.J. Salamo and R.R. Neurgaonkar, to be published in *Appl. Opt.*
13. W.W. Clark III, G.L. Wood, M.J. Miller, E.J. Sharp, G.J. Salamo, B.D. Monson and R.R. Neurgaonkar, submitted to *Appl. Opt.*
14. B.D. Monson, G.J. Salamo, A.G. Mott, M.J. Miller, E.J. Sharp, W.W. Clark III, G.L. Wood and R.R. Neurgaonkar, submitted to *Opt. Lett.*

Photorefractive Properties of Cr-doped Single Crystal Strontium Barium Niobate

Koichi Sayano, and Amnon Yariv
California Institute of Technology
Department of Applied Physics, 128-95
Pasadena, California 91125

Ratnakar R. Neurgaonkar
Rockwell International Science Center
P.O. Box 1085
Thousand Oaks, California 91360

Abstract

Cr-doped strontium barium niobate has shown significant reduction in the time of response compared to previously grown Ce-doped crystals, with room temperature response times as short as 0.2 sec. The experimental photorefractive two-beam coupling gain and response time of 1% and 1.6% Cr-doped SBN:60 and 1% Cr-doped SBN:75 will be presented and compared to results in Ce-doped SBN:60. The photorefractive effect in Cr-doped SBN:60 has also shown a strong temperature dependence, with gain increasing by a factor of two when the crystal was cooled from 40 to -20° C. Significant gain enhancement was also predicted and obtained by applying a DC electric field of up to 10 kV/cm.

1. Introduction

Ce-doped $\text{Sr}_{0.6}\text{Ba}_{0.4}\text{Nb}_2\text{O}_6$ (SBN:60) and $\text{Sr}_{0.75}\text{Ba}_{0.25}\text{Nb}_2\text{O}_6$ (SBN:75) have been shown to be effective media for optical processing and phase conjugation applications because of their large coupling constants, high optical quality, and relatively short response time.¹ In addition, the properties of SBN can be readily changed by varying its composition, large (~ 2 cm cube) crystals have been grown, it is more resistant to temperature changes, applied electric fields, and physical handling, and its open structure enables the addition of a variety of dopants.² The large photorefractive gain coefficients of materials like SBN and BaTiO_3 are desirable for high-efficiency devices and large optical amplification. However, another major goal is to reduce the response time of the materials for signal processing applications where speed is desired. In this paper, we present the results of Cr-doping in SBN:60 and SBN:75, which showed an almost order of magnitude decrease in the response time over Ce-doping, with a corresponding loss in gain by about a factor of 2.

2. Material Properties

SBN is a tungsten bronze ferroelectric material with a general formula of $\text{Sr}_x\text{Ba}_{1-x}\text{Nb}_2\text{O}_6$, with both $x = 0.6$ and $x = 0.75$ crystals having been successfully grown. The cation ratio x in large part determines its ferroelectric and electro-optic material properties. Table I shows some of these main properties of SBN:60 and SBN:75.^{2,3}

Table I: Properties of SBN:60 and SBN:75

Material	T_C $^{\circ}$ C	E-O Coeff (pm/V)	$n_i^3 r_{ij} / \epsilon_j$ (pm/V)	μ (cm^2/Vsec)	γ_R (cm^3/sec)
SBN:60	75	235	5.8	0.5	5×10^{-8}
SBN:75	56	1340	5.0	0.5	5×10^{-8}
BaTiO_3	128	1640	4.9	0.5	5×10^{-8}

Two Cr-doped SBN:60 samples, one with 1% and the other with 1.6% Cr in the flux, and one 1% Cr-doped SBN:75 sample were studied. All were grown using the Czochralski method and were poled into a single domain by

cooling through their cubic to ferroelectric phase transition temperatures with an applied electric field of 8 kV/cm along their c -axes.

Fig. 1 shows the absorption spectrum of the three Cr-doped SBN samples as well as that of Ce-doped SBN:60 for comparison. Ce-doped SBN:60 has a broad-band absorption level around 480 nm.¹ Cr-doped SBN has an additional absorption band centered around 650 nm, which may indicate a photoactive transition in the near infra-red.

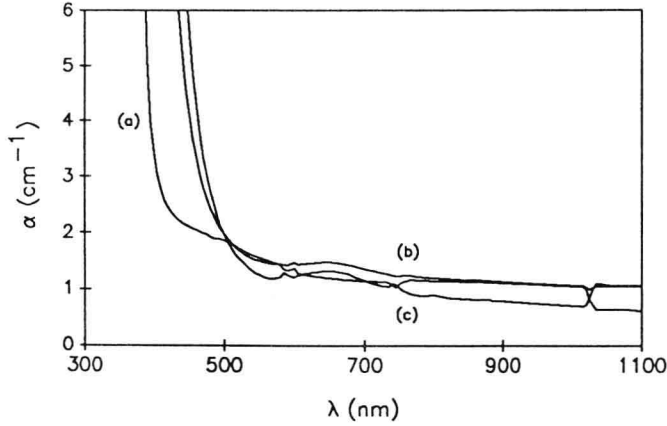


Fig. 1: Absorption spectrum for (a) Ce-doped SBN:60, (b) Cr-doped SBN:60, and (c) Cr-doped SBN:75.

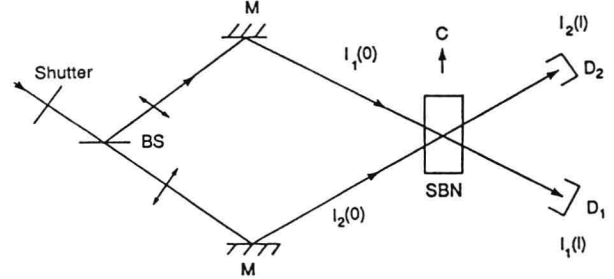


Fig. 2: Configuration of the two-beam coupling experiment used to characterize the SBN:60 crystals. The beam polarization was in the same plane as the c -axis. $I_1(0) + I_2(0)$ was approximately 0.25 W/cm².

3. Photorefractive Properties

The photorefractive properties of the SBN:60:Cr crystals were studied using two-beam coupling. Fig. 2 shows the experimental configuration used. Both beams were polarized in the direction of the c -axis, i.e. horizontally. The 514.5 nm line of an argon-ion laser with beam diameter of 0.3 cm was used. When the two beams intersect inside the crystal, energy is transferred from one beam to the other in the direction of the c -axis, which can be described by

$$\begin{aligned} I_1(z) &= I_1(0) \exp[-(\Gamma + \alpha)z] \\ I_2(z) &= I_2(0) \exp[(\Gamma - \alpha)z] \end{aligned} \quad (1)$$

where α is the absorption coefficient and Γ is the two-beam coupling constant, which is given by⁴⁻⁶

$$\Gamma \propto E_{sc} = iE_N \frac{E_0 + iE_d}{E_0 + i(E_d + E_N)} [1 - \exp(t/\tau)]. \quad (2)$$

The response time of the material is given by

$$\tau = t_0 \frac{E_0 + i(E_d + E_\mu)}{E_0 + i(E_d + E_N)} \quad (3)$$

where

$$t_0 = \frac{h\nu N_A}{sI_0(N_D - N_A)} \quad (4)$$

is the fundamental limit of the speed of the photorefractive effect.⁷ In the Eqns. (2) and (3), E_0 is the externally applied electric field, and the characteristic fields are given by

$$\begin{aligned} E_N &= \frac{eN_A}{\epsilon K} \left(1 - \frac{N_A}{N_D}\right) \approx \frac{eN_A}{\epsilon K} \text{ for } N_A \ll N_D \\ E_d &= \frac{k_B T K}{e} \\ E_\mu &= \frac{\gamma N_A}{\mu K}, \end{aligned} \quad (5)$$

where $K = 2\pi/\lambda_g$ is the wavenumber corresponding to the grating period, γ is the electron recombination rate, μ is the electron mobility, N_A is the trap density, N_D is the donor density, and s is the photoionization cross section.

Figs. 3 and 4 show the experimentally measured two-beam coupling constant and response time, respectively, of the Cr-doped SBN:60 and SBN:75 crystals along with Ce-doped SBN:60 for comparison as a function of the grating wavelength. By differentiating Eqn. (2), the trap density can be obtained as a function of the optimum grating wavelength for maximum Γ . The 1% Cr-doped crystal showed the fastest response time, around 0.2 sec, but had the smallest coupling constant, around 3 cm^{-1} . SBN:75 showed high gain even for a smaller E_{sc} due to its larger electro-optic coefficient.

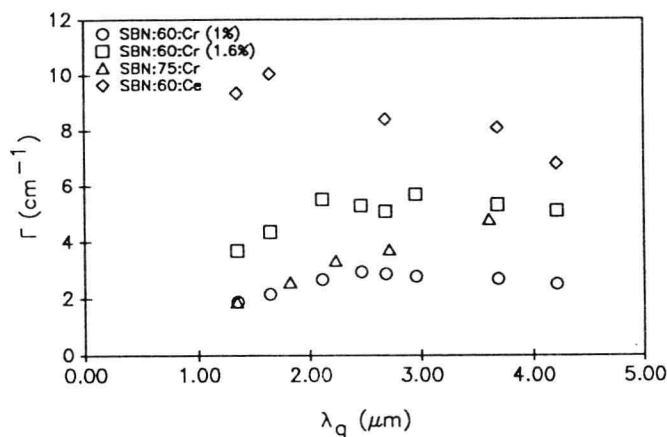


Fig. 3: Steady-state two-beam coupling constant Γ as a function of the grating period λ_g for SBN:60:Cr, doped with 1% Cr; SBN:60:Cr, doped with 1.6% Cr; SBN:75:Cr, doped with approximately 1% Cr; and SBN:60:Ce, doped with approximately 1% Ce.

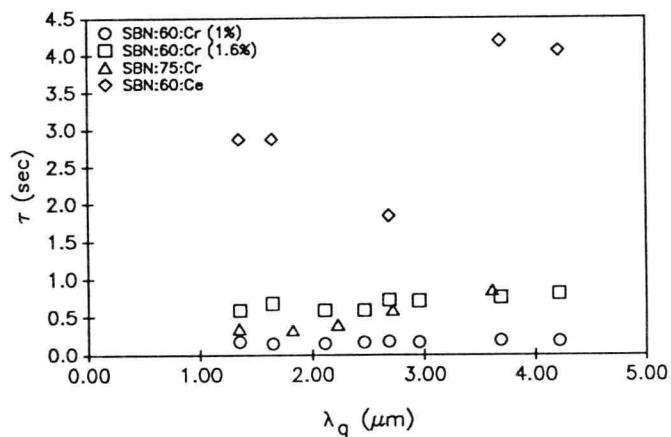


Fig. 4: Response times of the SBN:60:Cr, SBN:75:Cr, and SBN:60:Ce crystals as a function of grating period, for $\lambda = 514.5 \text{ nm}$ and $I_0 = 0.25 \text{ W/cm}^2$.

The preceding experiments were all performed using the 514.5 nm line of the argon-ion laser. These materials were found to be photorefractive at longer wavelengths as well. Figs. 5 and 6 show the effect of using the lower photon energy of the He-Ne laser for two-beam coupling measurements in a 1.6% Cr-doped SBN:60 at $\lambda_g = 2.46 \mu\text{m}$. Because of the lower absorption and fewer ionizable donors at the longer wavelength, the gain and response time results were predictably lower compared to identical measurements using the shorter wavelength sources. The absorption spectrum of Cr-doped SBN shows a broad-band absorption region in the red to near infra-red, and future investigation will determine whether these bands contribute to the photorefractive effect and whether or not these crystals are sensitive at the near infra-red wavelengths used by semiconductor lasers.

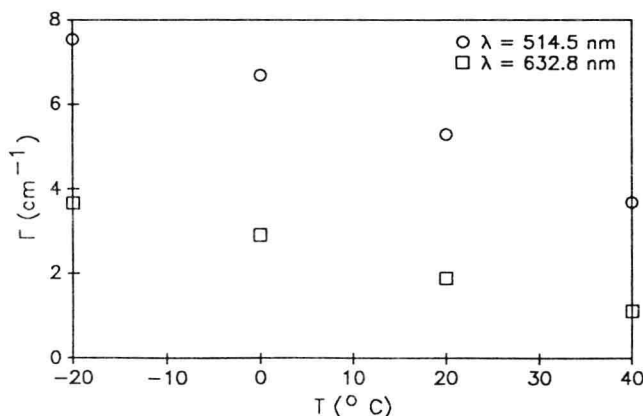


Fig. 5: Two-beam coupling constant of 1.6% Cr-doped SBN:60 at $\lambda = 514.5 \text{ nm}$ and 632.8 nm for $-20^\circ \text{C} \leq T \leq 40^\circ \text{C}$.

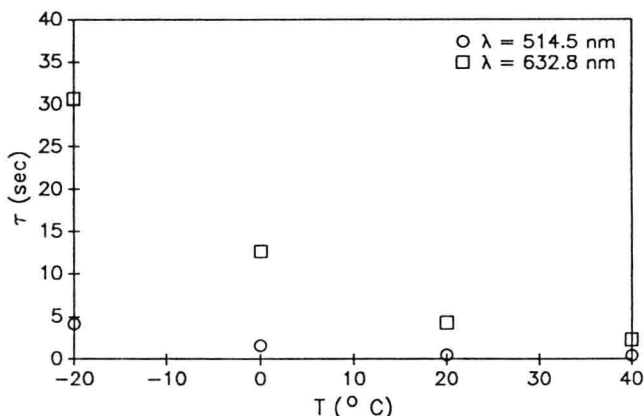


Fig. 6: Response time of 1.6% Cr-doped SBN:60 at $\lambda = 514.5 \text{ nm}$ and 632.8 nm for $-20^\circ \text{C} \leq T \leq 40^\circ \text{C}$.

4. Enhancement of Gain

Various methods are available for increasing the photorefractive gain of SBN. These include optimization of the grating period, lowering the temperature, and increasing the doping. Cooling Cr-doped SBN:60 has been found to increase gain, but results in a considerable increase of the response time, as shown in Figs. 5 and 6. This increase in Γ for lower temperatures can be attributed to decreased leakage of separated charges across the grating due to thermal excitation of trapped carriers.⁸ Increasing the doping is not too fruitful since E_{sc} tends to the smaller of E_d or E_N (see Eqn. (2)). In addition, there exists the practical problem of obtaining high optical quality crystals with large dopant concentrations.

Experimental results have shown that the application of an external DC field on Cr-doped SBN:60 results in a marked improvement in the photorefractive two-beam coupling constant. An external field tends to drive the excited electrons into their traps half a grating period away, resulting in a larger space charge field. In Eqn. (2), for $E_0 = 0$, the limiting field E_{sc} is the smaller of E_d and E_N . For large E_0 , the space charge field approaches E_N , which can be increased by increasing the trap density N_A .

Fig. 7 shows the experimental results of applying a DC field of up to 10 kV/cm to the 1% and 1.6% Cr-doped SBN:60 samples, where increases by more than a factor of two were realized. Since the two-beam coupling intensity gain is exponential, any increase in Γ results in a significant improvement in beam amplification and energy coupling in devices utilizing this effect. It would be possible to use thinner crystals of SBN in experiments and applications, or realize larger signal gain.

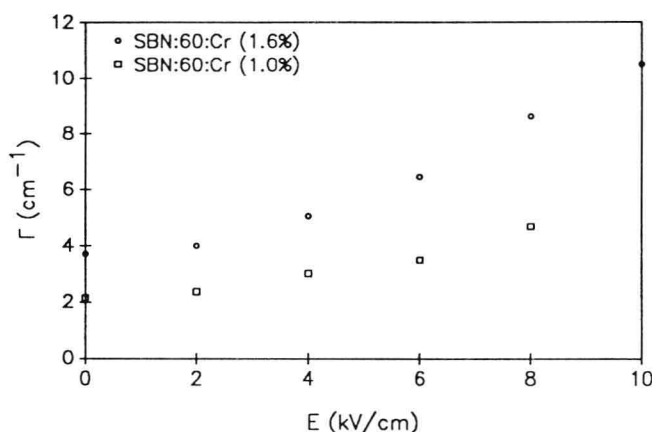


Fig. 7: Measured two-beam coupling constant of 1% and 1.6% Cr-doped SBN:60 with an applied electric field of $0 \leq E_0 \leq 10$ kV/cm.

5. Conclusions

Cr-doped SBN:60 has shown significant advantages in having a faster response over Ce-doped SBN. With the reduced response time, Cr-doped crystals had significantly lower photorefractive gain coefficients that previously grown Ce-doped ones. However, enhancement of the gain was possible through the application of an external DC electric field, resulting in increases in gain Γ by over a factor of two.

6. Acknowledgements

This work has been supported by grants from the Air Force Office of Scientific Research and the Army Research Office. K. Sayano also acknowledges partial support from the Air Force Weapons Laboratory Graduate Fellowship.

7. References

1. G.A. Rakuljic, A. Yariv, and R.R. Neurgaonkar, "Photorefractive properties of undoped, cerium-doped, and iron-doped single-crystal $\text{Sr}_{0.6}\text{Ba}_{0.4}\text{Nb}_2\text{O}_6$," *Opt. Eng.* **25**, pp. 1212-16 (1986).